Soluble epoxide hydrolase (*Ephx2*) silencing attenuates the hydrogen peroxide-induced oxidative damage in IEC-6 cells

Xiaohua Li[1], Xiaoqin Wu[2]

[1]Department of Anorectal Surgery, First People's Hospital of Yuhang District, Hangzhou, China
[2]Anorectal Care Unit, First People's Hospital of Yuhang District, Hangzhou, China

Submitted: 4 April 2018; **Accepted:** 30 July 2018
Online publication: 22 August 2019

Arch Med Sci 2021; 17 (4): 1075–1086
DOI: https://doi.org/10.5114/aoms.2019.87137

Corresponding author:
Xiaohua Li
Department of Anorectal Surgery
First People's Hospital of Yuhang District
Hangzhou, No. 369 Yingbin Road, Linping
Yuhang District, Hangzhou
Zhejiang 311000, China
Phone: 0571-89369917
E-mail: lixiaohua_xhl@163.com

Abstract

Introduction: Oxidative stress can cause intestinal disease. Soluble epoxide hydrolase (sEH, *Ephx2*) is related to cell apoptosis. The effect of *Ephx2* on the H_2O_2-induced oxidative damage remains unclear. Thus, we aimed to explore the effect of *Ephx2* on oxidative damage and the underlying potential mechanism.
Material and methods: The cell viability was determined using cell counting kit-8 (CCK-8) assay. The reactive oxygen species (ROS), apoptosis, and mitochondrial membrane potential (MMP) were examined using flow cytometry analysis. Commercial kits were applied to respectively determine the lactate dehydrogenase (LDH) leakage, malondialdehyde (MDA) content, and superoxide dismutase (SOD) activity. The expressions of target factors were measured by conducting quantitative reverse transcription-polymerase chain reaction (qRT-PCR) and western blot.
Results: We found that knockdown of *Ephx2* enhanced the viability of H_2O_2-treated IEC-6 cells, and that si-*Ephx2* reduced the ROS level, MMP loss, and apoptosis in comparison to the H_2O_2 model group. Knockdown of *Ephx2* was found to decrease LDH activity and MDA content, and to improve the SOD activity in comparison to those in the H_2O_2 model group. Knockdown of *Ephx2* reduced the expressions of Fas, Fasl, Bax, and cleavedcaspase-3 and elevated the expression of Bcl-2 in H_2O_2-treated IEC-6 cells. Furthermore, we observed that knockdown of *Ephx2* enhanced the phosphorylation of PI3K, Akt, and GSK3β, which were reduced by the treatment of H_2O_2. In addition, the anti-apoptotic effect of si-Ephx2 was enhanced in the presence of AUDA-pharmacological *Ephx2* inhibitor.
Conclusions: *Ephx2* silencing inhibited H_2O_2-induced oxidative damage. The PI3K/Akt/GSK3β pathway was related to the effect of si-*Ephx2*. Our study provided a potential target for the prevention of intestinal injury.

Key words: *Ephx2*, H_2O_2, oxidative damage, apoptosis.

Introduction

Reactive oxygen species (ROS) refers to a cluster of short-lived, highly reactive molecules; for example, peroxides, superoxide, hydroxyl free radical, and singlet oxygen. Caused by excessive ROS, oxidative stress can result in cell damage [1–3]. The over-accumulation of ROS in the gastrointestinal tract is considered to participate in the pathogenesis of intestinal diseases [4]. Intestinal epithelial cells (IECs) can act as a phys-

ical barrier in pathogen invasion [5]. It has been reported that intestinal epithelia damage may result from oxidative stress caused by increased ROS levels and collapsed antioxidant defences [6–9]. Thus, it is crucial to preserve physiological redox balance, and this balance can alleviate tissue injury in diseases characterised by pathologic oxidative stress.

Apoptosis can be triggered by the death receptor pathway and the mitochondrial pathway [10]. Research revealed that PI3K/Akt signal pathway could inhibit apoptosis and promote cell viability [11]. The phosphatidylinositol 3-kinase (PI3K)-dependent production of phosphatidylinositol-triphosphate (PIP3) helps protect cells from apoptotic cell death [12]. Protein kinase B (Akt), a direct downstream target of PI3K, can be activated by PIP3 [13]. The p-Akt can phosphorylate glycogen synthase kinase 3β (GSK3β), which can regulate many cellular functions, including apoptosis [14, 15]. Furthermore, a recent study has proven that GSK3β can regulate key steps in both the mitochondrial pathway and the death receptor pathways [16].

Soluble epoxide hydrolase (sEH, *Ephx2*) is a major enzyme that metabolises epoxyeicosatrienoic acids (EETs) to dihydroxyeicosatrienoic acids [17, 18]. An increasing number of studies have pointed out that EETs could suppress apoptosis [19–25]. It is suggested that the *Ephx2* inhibition might also be related to cell apoptosis. Moreover, it has been reported that several signalling pathways, including PI3K/Akt, also take part in producing the anti-apoptotic effects of EETs [26]. However, to the best of our knowledge, whether *Ephx2* silencing could attenuate the oxidative damage remains unclear. Thus, this study aimed to explore the effect of *Ephx2* silencing on the H_2O_2-induced oxidative damage in IECs.

Material and methods

Cell culture

IEC-6 cells (rat-derived intestinal epithelial cells) were purchased from the American Type Culture Collection (ATCC, CRL-1592, Manassas, VA, USA). Cells were maintained in Dulbecco's Modified Eagle's Medium (DMEM, Thermo Scientific) containing 10% fetal bovine serum (FBS, Thermo Scientific, UT, USA), 100 mg/ml of streptomycin, and 100 U/ml of penicillin (Cologne Gmbh, Germany) at 37°C with 5% CO_2 in an incubator. After being cultured for 24 h, the morphology of cells was observed by an inverted microscope (Olympus optical).

Cell transfection and grouping

Cells (~4 × 10^5) were seeded in six-well plates. After being cultured for 24 h, the medium was replaced with Opti-MEM (Invitrogen, Grand Island, NY, USA) and the plasmids were transfected following Lipofectamine 2000 protocol (Invitrogen). The pSUPER vector (Oligoengine, Seattle, WA) was used for small interfering RNA against *Ephx2* (si-*Ephx2*). Next, after being incubated for 48 h, the treated cells were divided into six groups as follows: control group (cells with no treatment); NC group (cells transfected with negative vector); H_2O_2 model group (cells treated with 100 μM H_2O_2 for 12 h); NC + H_2O_2 group (cells transfected with empty vector and treated by 100 μM H_2O_2 for 12 h); and si-*Ephx2* + H_2O_2 group (cells transfected with siRNA-*Ephx2* and treated by 100 μM H_2O_2 for 12 h). The 12-(3-adamantan-1-yl-ureido)-dodecanoicacid (AUDA) was purchased from Cayman. The stock solution was prepared in dimethyl sulphoxide (DMSO). According to previous studies [27, 28], the concentration of AUDA was selected as 5 μM and the incubation duration was set for 15 min.

Cell counting kit-8 assay

Cells (2 × 10^5) were cultivated in 96-well plates, and cell viability was detected using Cell Counting Kit-8 (CCK-8) (Beyotime, Beijing, China). After performing H_2O_2 treatment and transfection, the CCK-8 was added and incubated for another 3 h at 37°C. The absorbance was measured at 450 nm using a MultiSkan 3 ELISA Reader (Thermo Fisher Scientific, USA).

Determination of reactive oxygen species and mitochondrial membrane potential

The ROS production was detected using 2',7'-dichlorodihydrofluorescein diacetate (DCFH-DA, Sigma-Aldrich, Merck KGaA). The cells were stained with DCFH-DA at 37°C for 30 min. In the presence of ROS, DCFH-DA was transformed into DCF, which can give a fluorescent signal. The fluorescence of DCF reflected the ROS level. The changes in mitochondrial membrane potential (MMP) were detected using Rhodamine 123 dye (Sigma Aldrich, Merck KGaA), which can penetrate the cell membrane. The cells were stained with Rhodamine 123 (10 μg/ml) at 37°C for 30 min without light. Next, the fluorescence was measured using flow cytometry (Guava Technologies, Inc., Millipore, USA). 1 μM AUDA (Cayman, USA) was used to treat the cells at 37°C for 2 h in order to test the function verification of *Ephx2*.

Detection of cell apoptosis using flow cytometry

Cell apoptosis in each group was analysed using flow cytometry (Guava Technologies, Inc.), according to the protocol of the Annexin V-FITC/PI Apoptosis Detection kit (KeyGEN Biotechnology, Nanjing, China). Data were analysed by FCS

Express V3 software (De Novo Software, Los Angeles, CA). By using Annexin V-FITC/PI double fluorescent staining, cells in each group were identified as follows: unlabelled viable cells, Annexin V-FITC-bound cells (early apoptotic cells), PI-stained cells (necrotic cells), and double-labelled cells (late apoptotic cells). Annexin V-positive cells were considered as the apoptotic population.

Determination of lactate dehydrogenase, methane dicarboxylic aldehyde, and superoxide dismutase

The lactate dehydrogenase (LDH) release, methane dicarboxylic aldehyde (MDA) content, and superoxide dismutase (SOD) activity were determined using LDH assay kit, MDA assay kit (TBA method), and superoxide dismutase (SOD) assay kit (WST-1 method) (all purchased from the Institute of Jiancheng Bioengineering, Nanjing, China), following the manufacturer's protocol. The activity of LDH was shown as U/l. The content of MDA was expressed as μM/g protein, while the activity of SOD was expressed as U/l. The absorbance was measured using a Multiskan MK3 microplate reader (Thermo Fisher Scientific, Inc.).

Quantitative reverse transcription-polymerase chain reaction (qRT-PCR)

The total RNA of cells (5×10^5) in each group was extracted using Trizol reagent (Invitrogen, Carlsbad, CA). Briefly, chloroform (200 μl) was added after the cells had been homogenised in TRIZol reagent (1 ml). Next, the samples were incubated at room temperature for 2 min. After being centrifuged (12,000 g at 4°C for 15 min), the supernatant was carefully drawn into a new tube. The ice isopropyl alcohol was added and incubated at room temperature for 20 min. Posterior to the centrifugation (12,000 g at 4°C for 10 min) the supernatants were removed completely and the precipitate was washed twice by 75% ethanol. Finally, nuclease-free water was added to elute the RNA. The concentration and purity were detected using NanoDrop 2000 (Thermo Fisher Scientific, Waltham, MA, USA). Next, cDNA was obtained by conducting reverse transcription with FastQuant RT Kit (Tiangen, China), according to the manufacturer's protocol. In total, 2 μg RNA was incubated with 5 × g DNA buffer (total 10 μl) at 42°C for 3 min. The mixture (FQ-RT Primer Mix, 10 × fast RT buffer and RT enzyme mix) was then added and incubated first at 42°C for 15 min and then at 95°C for 5 min. The obtained cDNAs were prepared for conduction of qPCR and the reactions were performed in the ABI 7500 real-time PCR system (Applied Biosystems, Foster City, CA, USA) under the following conditions: 95°C for 5 min, 40 cycles at 95°C for 15 s, at 60°C for 20 s, and at 72°C for 15 s. GAPDH served as a reference gene, and data analyses were performed by the $2^{-\Delta\Delta Ct}$ method. The specific primers were used as in Table I. Each sample was detected at least three times.

Western blotting

The cells were lysed by NP40 lysis buffer (Beyotime, Beijing, China). Lysates were incubated on ice for 30 min and then sonicated for 15 s twice. The protein concentrations were determined using BCA protein assay kit (CWBIO, China). Total proteins were separated by 10% SDS-PAGE gel and then transferred onto polyvinylidene difluoride membranes (GE Healthcare, Little Chalfont, UK). After being blocked with 5% skimmed milk solution for 1 h, the membranes were incubated overnight at 4°C with the following primary antibodies: anti-sEH (1 : 100, Cayman Chemical), anti-GAPDH (1 : 500, Santa Cruz Biotechnology), anti-Fas, anti-Fasl (1 : 500, Bioworld Technology, Inc., Louis Park, MN), anti-Bcl-2, anti-Bax (1 : 500, Abcam, Cambridge, USA), anti-cleavedcaspase-3 (1 : 500, Abcam, Cambridge, USA), anti-p-PI3K p85-α (phospho Y607) (1 : 500, abcam, USA), anti-PI3K (1 : 500, Abcam, USA), anti-p-Akt (phospho S473) (1 : 500, Cell Signaling Technology, Danvers, USA), anti-Akt (1 : 1000, Cell Signaling Technology, USA), anti-GSK3β (1 : 1000, Cell Signaling Technology, USA), and anti-p-GSK3β (phospho S9) (1 : 1000, Abcam, USA). Next, the membranes were incubated with HRP-conjugated secondary antibodies (1 : 3000, Zhongshan Golden Bridge Biotechnology, Beijing, China). The bands were determined using a Molecular Imager VersaDoc MP 5000 System

Table I. Primers for the qPCR

Gene	Forward primers (5'-3')	Reverse primers (5'-3')
Ephx2	AAGATTTAGCCAGTGGCGTGTC	ATCACTGCTGGCAAAAGAACG
Fas	TATCACCACTATTGCTGGAGTCATG	TCAATGTGTCATACGCTTCTTTCTT
Fasl	CTCTGGAATGGGAAGACACCTATG	GCAAGATTGACCCCGGAAGTATA
Bcl-2	GGAGCGTCAACAGGGAGATGT	GCCAGGAGAAATCAAACAGAGG
Bax	GCGAATTGGAGATGAACTGGAC	CTAGCAAAGTAGAAGAGGGCAACC
GADPH	CCAGCCTCGTCCCGTAGAC	ATGGCAACAATCTCCACTTTGC

(Bio-Rad, Hercules, CA). The densitometry was determined using a Quantity One (Bio-Rad).

Statistical analysis

Data are shown as the mean ± SEM. All statistical analyses were performed using SPSS software (version 15.0, SPSS, Chicago, IL, USA). One-way analysis of variance (ANOVA) following Turkey's test was performed to study statistical differences among groups. A value of $p < 0.05$ was considered as statistically significant.

Availability of data and material

The analysed datasets generated during the study are available from the corresponding author upon reasonable request.

Results

Ephx2 silencing improved viability of intestinal epithelial cells induced by H_2O_2

The IEC-6 cells were observed under an inverted microscope (Figure 1 A). The efficiency of transfection was confirmed by an obvious inhibition of the *Ephx2* at protein and the mRNA levels (Figures 1 B, C). The cells were also treated with 100 μM H_2O_2 for 48 h, and the results showed that the cell viability was reduced by H_2O_2 in a time-dependent manner. However, the knockdown of *Ephx2* rescued the viability of the H_2O_2-treated cells. After being incubated with H_2O_2 for 12 h, the cell viability was decreased by nearly 30%. Thus, 12-h incubation with 100 μM H_2O_2 was set as the condition for inducing cell injury in the subsequent experiments (Figure 1 D).

Ephx2 silencing attenuated reactive oxygen species accumulation, suppressed apoptosis, and recovered mitochondrial membrane potential in IEC-6 cells

The knockdown of *Ephx2* was found to markedly reduce the H_2O_2-induced ROS generation (Figure 2 A). Furthermore, the inhibition of *Ephx2* evidently improved the level of MMP impaired by H_2O_2 (Figure 2 B). Meanwhile, when the cells were exposed to H_2O_2, we found that the total apoptotic cells were increased by approximately 20%, while *Ephx2* silencing inhibited cell apoptosis by about 13% (Figure 2 C).

Effects of *Ephx2* silencing on the lactate dehydrogenase leakage, methane dicarboxylic aldehyde level, and superoxide dismutase activity

The LDH release, MDA content, and SOD activity were measured in order to evaluate the role of *Ephx2* inhibition in H_2O_2-induced oxidative stress. An evident increase of LDH leakage was observed in IECs treated by H_2O_2, compared with the control group. However, *Ephx2* silencing reduced the LDH release (Figure 2 D). Similarly, noticeably increased levels of MDA induced by H_2O_2 could be mitigated by *Ephx2* inhibition (Figure 2 E). Additionally, the activity of SOD clearly decreased in the H_2O_2 model group. However, *Ephx2* silencing could partly recover the decreased content of SOD (Figure 2 F).

Ephx2 silencing regulated the apoptosis-related molecules in intestinal epithelial cells

We detected several apoptotic molecules in order to explore the role of *Ephx2* inhibition in the apoptosis. The mRNA levels of Fas (Figure 3 A), Fasl (Figure 3 B), and Bax (Figure 3 C) were increased by H_2O_2. We found that the expression of Bcl-2 (Figure 3 D) was decreased by H_2O_2 and was then reversed by *Ephx2* knockdown. Also, the western blot results showed similar protein expressions (Figures 3 E–I), and the protein level of cleaved caspase-3 was increased by H_2O_2 and inhibited by *Ephx2* silencing (Figure 3 J).

Ephx2 silencing enhanced the levels of p-PI3K, p-Akt, and p-GSK3β

To further study the potential mechanism of *Ephx2* in H_2O_2-induced IECs, the proteins expressions of p-PI3K (phospho Y607), PI3K, p-Akt (phospho S473), Akt, p-GSK3β (phospho S9), and GSK3β were determined in IEC-6 cells. We found that *Ephx2* knockdown remarkably raised the ratios of the p-PI3K/ PI3K (Figure 4 A), p-Akt/Akt (Figure 4 B), and p-GSK3β/GSK3β (Figure 4 C), compared to H_2O_2.

AUDA reduced the apoptosis of intestinal epithelial cells caused by H_2O_2

12-(3-adamantan-1-yl-ureido)-dodecanoic acid (AUDA) is considered as a pharmacological inhibitor of *Ephx2* [28]. Therefore, we used AUDA to further prove the effect of *Ephx2*. As shown in Figure 5, we found that H_2O_2 induced apoptosis of IECs. However, the treatment of AUDA or si-*Ephx2* reduced the apoptosis of IECs in comparison to that in the H_2O_2 group. Moreover, the combined treatment of AUDA and si-*Ephx2* was found to produce a synergy effect on inhibiting H_2O_2-induced apoptosis in IECs.

Discussion

Researchers found that H_2O_2 could induce oxidative stress in cells, therefore leading to apoptosis [29]. Soluble epoxide hydrolase (sEH) is encoded by *Ephx2* gene. A previous study pointed out

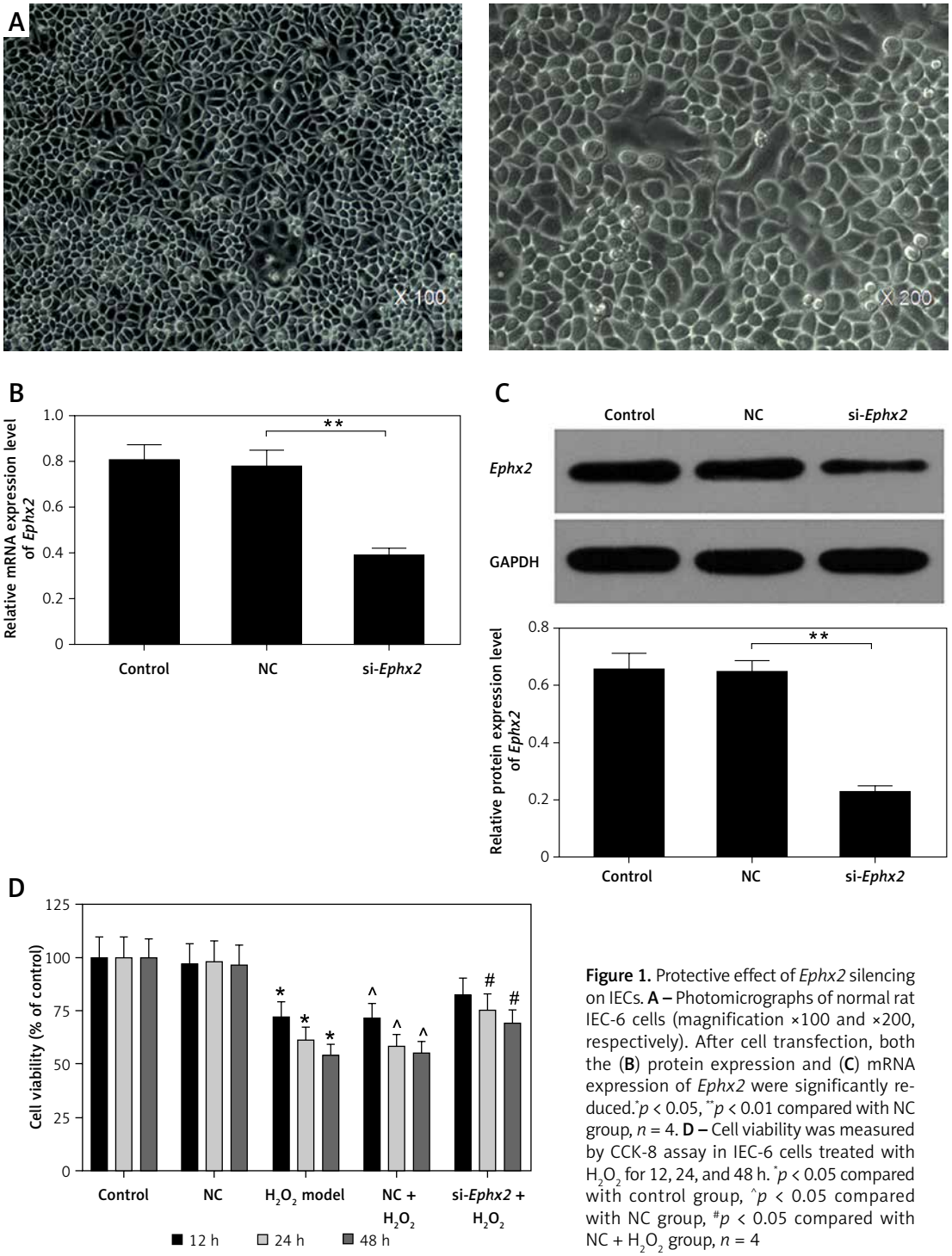

Figure 1. Protective effect of *Ephx2* silencing on IECs. **A –** Photomicrographs of normal rat IEC-6 cells (magnification ×100 and ×200, respectively). After cell transfection, both the (**B**) protein expression and (**C**) mRNA expression of *Ephx2* were significantly reduced. $^{*}p < 0.05$, $^{**}p < 0.01$ compared with NC group, $n = 4$. **D –** Cell viability was measured by CCK-8 assay in IEC-6 cells treated with H_2O_2 for 12, 24, and 48 h. $^{*}p < 0.05$ compared with control group, $^{\wedge}p < 0.05$ compared with NC group, $^{\#}p < 0.05$ compared with NC + H_2O_2 group, $n = 4$

that *Ephx2*-knockout mice did not develop heart failure and arrhythmia [30]. Studies also showed that specific sEH inhibitors could decrease blood pressure and repair damage in some organs, for example in heart, kidney, or vessels [31, 32]. Thus, it is interesting to explore the role of *Ephx2* gene in H_2O_2-induced IEC injury. In this study, we found that *Ephx2* silencing could attenuate H_2O_2-induced oxidative damage in intestinal epithelial cells. Moreover, *Ephx2* inhibition was found to reduce the ROS level and apoptosis rate and reserved the MMP loss. In addition, our results showed *Ephx2* silencing increased the expressions of Fas, Fasl, and Bax. By contrast, *Ephx2* silencing inhibited the expressions of Bcl-2 and cleaved caspase-3. Furthermore, *Ephx2* silencing might enhance the phosphorylation of PI3K, Akt, and GSK3β.

Researchers also reported that inhibiting soluble epoxide hydrolase (sEH) or knocking down *Ephx2* could prevent islet cell apoptosis [33]. An-

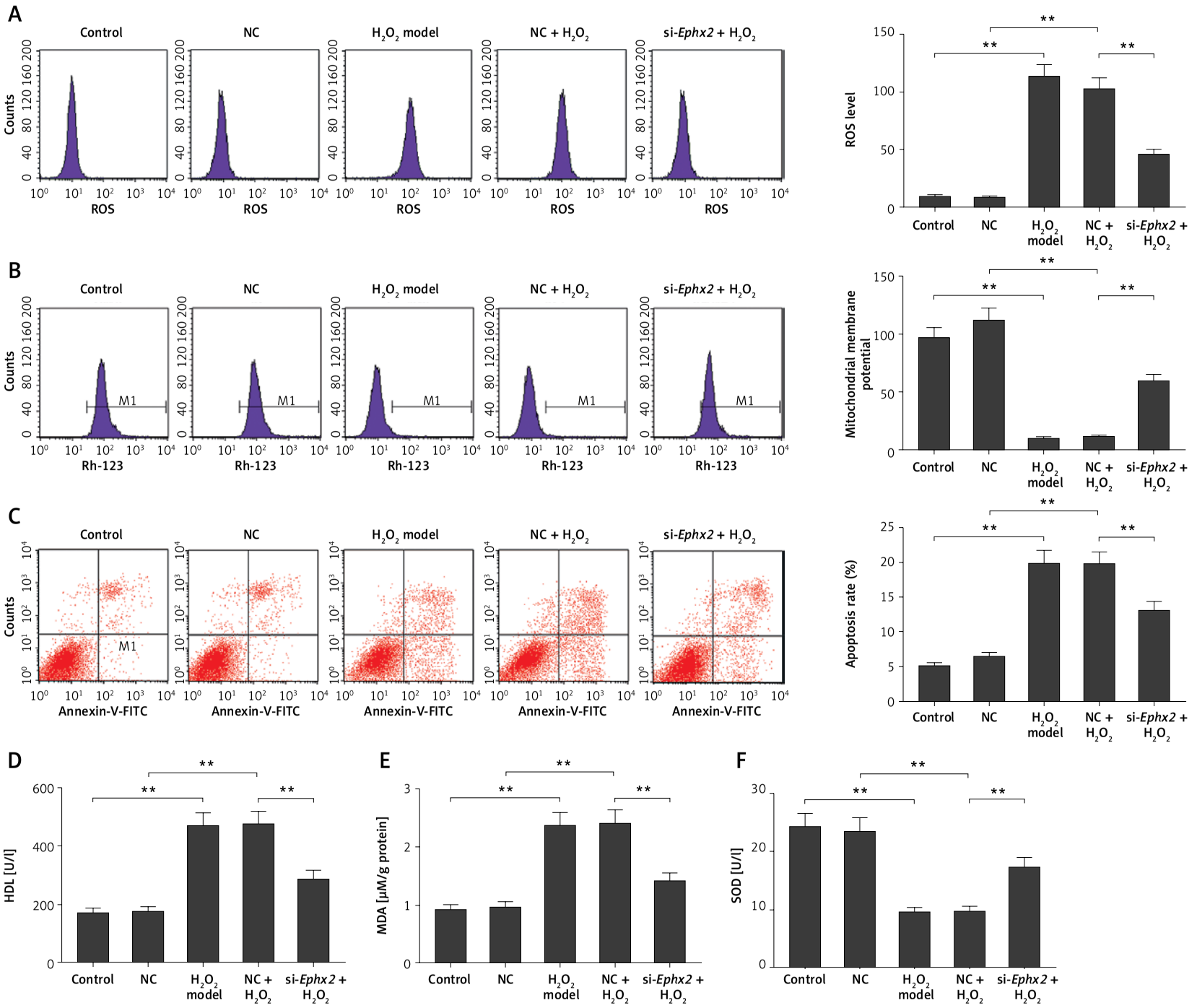

Figure 2. *Ephx2* silencing attenuated H_2O_2-induced oxidative damage. **A** – ROS fluorescence intensity was detected by flow cytometry. **B** – Changes of MMP in each group were measured by flow cytometry. **C** – Apoptosis rate was measured by flow cytometry, and the apoptotic cell number was quantitatively counted. The LDH release (**D**), MDA (**E**) content, and SOD (**F**) activity in H_2O_2-induced IECs were determined by spectrophotometry. **referred to $p < 0.01$, $n = 4$

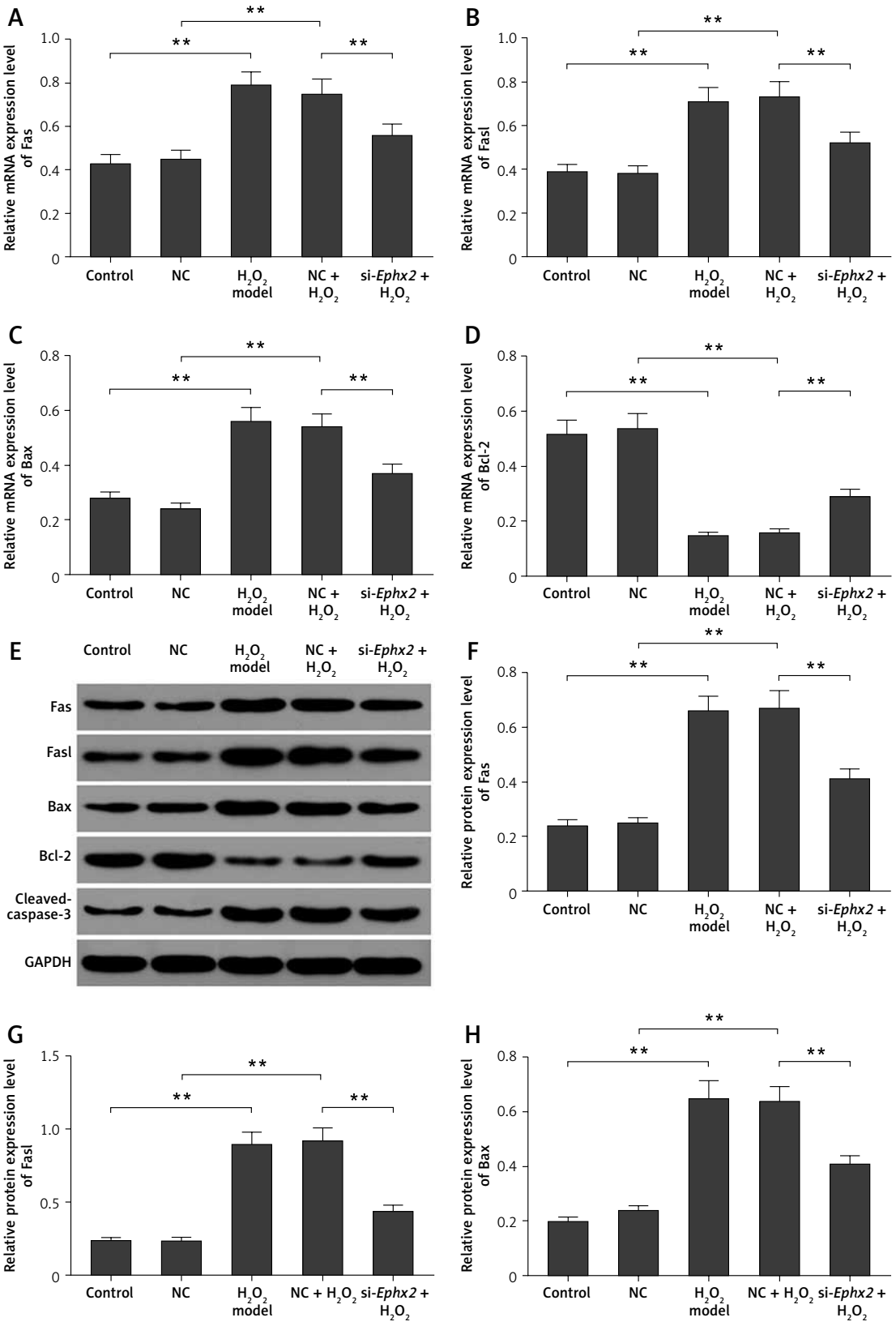

Figure 3. Effect of *Ephx2* silencing on the expressions of apoptosis-related molecules in H_2O_2-induced IECs. The mRNA expressions of Fas (**A**), Fasl (**B**), Bax (**C**), and Bcl-2 (**D**) were detected by qPCR. **E –** The protein levels of apoptosis-related molecules were detected by western blot assays and the relative quantification was calculated (**F–J**). **Referred to $p < 0.01$, $n = 4$

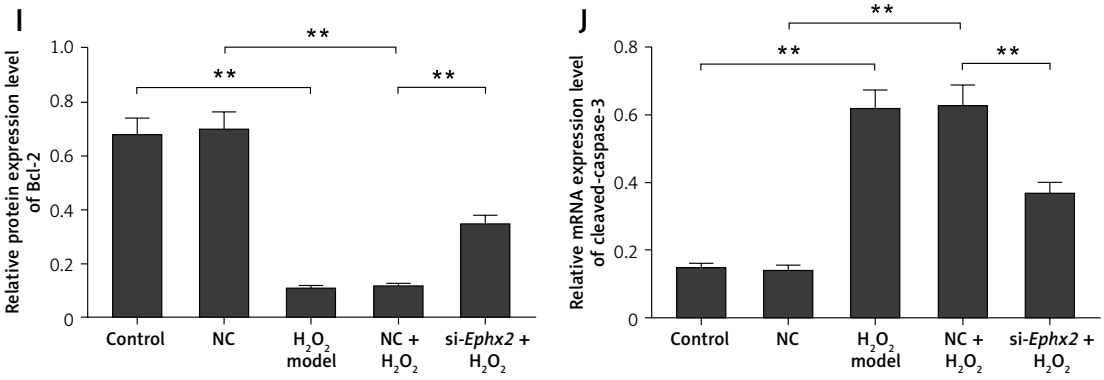

Figure 3. Cont.

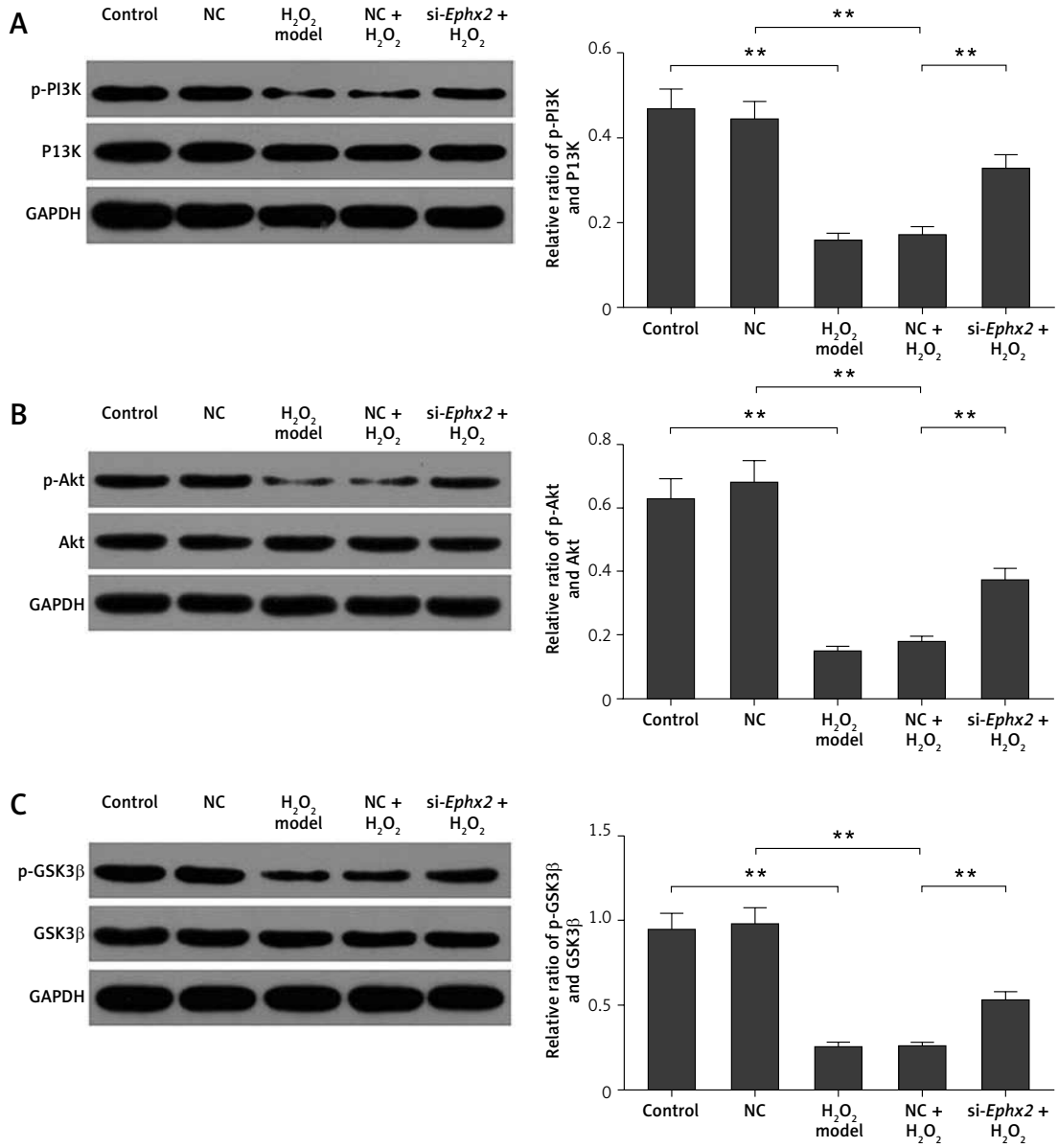

Figure 4. *Ephx2* silencing increased the ratios of p-PI3K/PI3K, p-Akt/Akt, and p-GSK3β/GSK3β in H_2O_2-induced IECs. **A –** Relative ratio of p-PI3K/PI3K in IECs. **B –** Relative ratio of p-Akt/Akt in IECs. **C –** Relative ratio of p-GSK3β/GSK3β in IECs. **referred to $p < 0.01$, $n = 4$

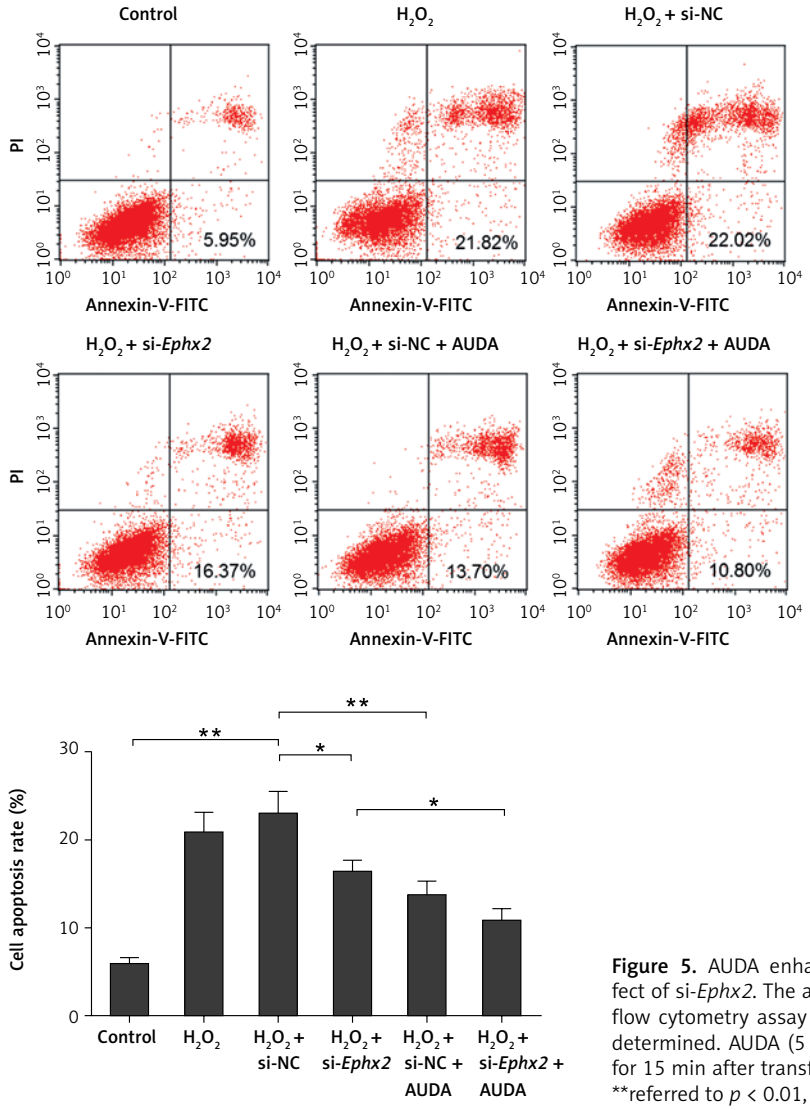

Figure 5. AUDA enhanced the anti-apoptotic effect of si-*Ephx2*. The apoptosis was determined by flow cytometry assay and the apoptosis rate was determined. AUDA (5 μM) was used to treat cells for 15 min after transfection. *referred to $p < 0.05$, **referred to $p < 0.01$, $n = 4$

other study also found that excessive H_2O_2 in intestinal epithelial cells contributed to the damage of colonic barrier function structures [5]. In this study, we found that *Ephx2* silencing could improve the viabilities of IECs that were treated with H_2O_2. As a major component of ROS, H_2O_2 can induce apoptosis of different cell types [34]. In cells, H_2O_2 can trigger the overproduction of intracellular ROS, leading to the MMP loss [35]. The collapsed MMP can release cytochrome c, therefore causing apoptosis [36]. Our results showed that H_2O_2 could improve ROS accumulation, reduce MMP, and increase the apoptosis rate, suggesting that *Ephx2* inhibition might attenuate H_2O_2-induced apoptosis in IECs.

Lactate dehydrogenase is associated with cell viability and membrane integrity, and MDA is the production of lipid peroxidation and can be used to evaluate oxidative stress [37, 38]. Our results showed that the LDH leakage was extended by H_2O_2 treatment, suggesting that H_2O_2 could impair cellular membranes and cause LDH leakage. We also found that *Ephx2* silencing could attenuate the increased LDH release and reverse the MDA activity. As one of the main antioxidant enzymes, SOD produced a protective effect on the oxidative stress-induced injury by eliminating ROS [39]. During the experiment, IEC in combination with *Ephx2* silencing was found to recover the decreased SOD activity, which was induced by H_2O_2. These results suggested that *Ephx2* silencing might alleviate the H_2O_2-induced oxidative damage.

The impairment of MMP and ROS generation was believed to be able to contribute to apoptotic signalling in multiple cells [40]. Apoptosis is caused via the extrinsic and intrinsic pathways [41]. The former could be initiated mainly by Fas and Fas ligand (Fasl), which can ultimately activate caspase-3, therefore causing apoptosis [42]. The latter can be regulated by the Bcl-2 family including Bcl-2 (anti-apoptotic gene) and Bax (pro-apop-

totic gene) [43, 44]. The crumble mitochondrial membrane caused by radiation and free radicals can release a pro-apoptosis protein cytochrome c from mitochondria to cytosol [45, 46]. The release of cytochrome c into the cytosol can activate procaspase-9 by forming the apoptosome, and then the cleaved caspase-9 will regulate the activity of caspase-3 [47]. In the final stage, both pathways initiated the apoptosis by activating effect or caspases such as caspase-3 [48]. We found that H_2O_2 increased the expression levels of Fas, Fasl, Bax, and cleaved caspase-3 but reduced Bcl-2 expression. However, *Ephx2* silencing could suppress the Fas, Fasl, Bax, and cleaved caspase-3 expressions and enhance the level of the Bcl-2. This phenomenon indicated that the inhibition of *Ephx2* might suppress the H_2O_2-induced apoptosis.

Apoptotic induced by H_2O_2 may activate the PI3K/Akt pathway, which functions critically in IEC survival and differentiation [49]. The p-Akt promotes cell survival by phosphorylation and inactivation of pro-apoptosis molecules such as GSK3β [50]. Moreover, p-Akt directly phosphorylates GSK3β at Ser9. This phosphorylation negatively regulates the kinase activity of GSK3β. Thereafter, p-GSK3β can suppress the opening of mitochondrial permeability transition pores [51]. Sustained inhibition of GSK3β is associated with the attenuation of apoptosis [52]. Moreover, Bax is considered as a direct target of GSK3β, the inhibition of which could promote Bcl-2 expression [53, 54]. In this study, we found that the expressions of p-PI3K (phospho Y607), p-Akt (phospho S473), and p-GSK3β (phospho S9) were decreased by H_2O_2 treatment. It has been reported that the PI3K-dependent GSK3β-phosphorylation is pertinent to intestinal epithelial cell wound-healing and repair. Noticeably, the wounding induces the expression of p-GSK3β mediated by PI3K [55], suggesting that the phosphorylation of PI3K can help protect against epithelial cell injury. In our study, *Ephx2* silencing improved the ratios of p-PI3K/PI3K, p-Akt/Akt, and p-GSK3β/GSK3β, compared to the H_2O_2 model group. These data suggest that the knockdown of *Ephx2* protects the epithelial cells from H_2O_2 -induced injury. As a pharmacological *Ephx2* inhibitor [29], AUDA could stabilise and increase the epoxyeicosatrienoic acids levels and is increasingly used in various diseases models [56] to further investigate the role of *Ephx2* in H_2O_2-treated IECs. The results showed that the treatment of AUDA inhibited the apoptosis caused by H_2O_2. These data further proved the protective role of si-*Ephx2* in IECs.

In conclusion, we found that *Ephx2* silencing could attenuate H_2O_2-induced oxidative damage in intestinal epithelial cells by suppressing ROS levels. We also found that *Ephx2* silencing could inhibit the loss of MMP and regulate the levels of apoptosis-related molecules so as to reduce the apoptosis of IECs, and that *Ephx2* silencing might enhance the phosphorylation of PI3K, Akt, and GSK3β. Furthermore, the inhibitor of Ephx2 was observed to be able to reduce H_2O_2-induced IECs injury. These results showed a possible mechanism of the anti-apoptosis effect of *Ephx2* inhibition.

Conflict of interest

The authors declare no conflict of interest.

References

1. Redza-Dutordoir M, Averill-Bates DA. Activation of apoptosis signalling pathways by reactive oxygen species. Biochim Biophys Acta 2016; 1863: 2977-92.
2. Brieger K, Schiavone S, Miller FJ Jr, Krause KH. Reactive oxygen species: from health to disease. Swiss Medical Weekly 2012; 142: w13659.
3. Majer M, Gackowski D, Różalski R, Siomek-Górecka A, Oliński R, Budzyński J. Systemic oxidoreductive balance and vascular function in individuals without clinical manifestation of atherosclerosis. Arch Med Sci Atheroscler Dis 2017; 2: e37-e45.
4. Bhattacharyya A, Chattopadhyay R, Mitra S, Crowe SE. Oxidative stress: an essential factor in the pathogenesis of gastrointestinal mucosal diseases. Physiol Rev 2014; 94: 329-54.
5. Gu BH, Minh NV, Lee SH, et al. Deoxyschisandrin inhibits H_2O_2-induced apoptotic cell death in intestinal epithelial cells through nuclear factor-kappaB. Int J Mol Med 2010; 26: 401-6.
6. Kim YJ, Kim EH, Hahm KB. Oxidative stress in inflammation-based gastrointestinal tract diseases: challenges and opportunities. J Gastroenterol Hepatol 2012; 27: 1004-10.
7. Ozsurekci Y, Aykac K. Oxidative stress related diseases in newborns. Oxid Med Cell Longev 2016; 2016: 2768365.
8. Alzoghaibi MA. Concepts of oxidative stress and antioxidant defense in Crohn's disease. World J Gastroenterol 2013; 19: 6540-7.
9. Stojiljković V, Pejić S, Kasapović J, et al. Glutathione redox cycle in small intestinal mucosa and peripheral blood of pediatric celiac disease patients. An Acad Bras Cienc 2012; 84: 175-84.
10. Zeng L, Li T, Xu DC, et al. death receptor 6 induces apoptosis not through type I or type II pathways, but via a unique mitochondria-dependent pathway by interacting with Bax protein. J Biol Chem 2012; 287: 29125-33.
11. Chao X, Zao J, Xiao-Yi G, Li-Jun M, Tao S. Blocking of PI3K/AKT induces apoptosis by its effect on NF-κB activity in gastric carcinoma cell line SGC7901. Biomed Pharmacother 2010; 64: 600-4.
12. Maddika S, Ande SR, Wiechec E, Hansen LL, Wesselborg S, Los M. Akt-mediated phosphorylation of CDK2 regulates its dual role in cell cycle progression and apoptosis. J Cell Sci 2008; 121: 979-88.
13. Dijkers PF, Birkenkamp KU, Lam WF, et al. FKHR-L1 can act as a critical effector of cell death induced by cytokine withdrawal: protein kinase B-enhanced cell survival through maintenance of mitochondrial integrity. J Cell Biol 2002; 156: 531-42.
14. Song G, Ouyang G, Bao S. The activation of Akt/PKB signaling pathway and cell survival. J Cell Mol Med 2005; 9: 59-71.

15. Woodgett JR, Ohashi PS. GSK3: an in-Toll-erant protein kinase? Nat Immunol 2005; 6: 751-2.
16. Chen L, Xiang Y, Kong L, et al. Hydroxysafflor yellow A protects against cerebral ischemia-reperfusion injury by anti-apoptotic effect through PI3K/Akt/GSK3β pathway in rat. Neurochem Res 2013; 38: 2268-75.
17. Wang YX, Ulu A, Zhang LN, Hammock B. Soluble epoxide hydrolase in atherosclerosis. Curr Atheroscler Rep 2010; 12: 174-83.
18. Wang ZH, Davis BB, Jiang DQ, Zhao TT, Xu DY. Soluble epoxide hydrolase inhibitors and cardiovascular diseases. Curr Vasc Pharmacol 2013; 11: 105-11.
19. Chen C, Li G, Liao W, et al. Selective inhibitors of CYP2J2 related to terfenadine exhibit strong activity against human cancers in vitro and in vivo. J Pharmacol Exp Ther 2009; 329: 908-18.
20. Chen C, Wei X, Rao X, et al. Cytochrome P450 2J2 is highly expressed in hematologic malignant diseases and promotes tumor cell growth. J Pharm Exp Ther 2011; 336: 344-55.
21. Ma J, Zhang L, Han W, et al. Activation of JNK/c-Jun is required for the proliferation, survival, and angiogenesis induced by EET in pulmonary artery endothelial cells. J Lipid Res 2012; 53: 1093-105.
22. Ma J, Zhang L, Li S, et al. 8,9-Epoxyeicosatrienoic acid analog protects pulmonary artery smooth muscle cells from apoptosis via ROCK pathway. Exp Cell Res 2010; 316: 2340-53.
23. Batchu SN, Lee SB, Qadhi RS, et al. Cardioprotective effect of a dual acting epoxyeicosatrienoic acid analogue towards ischaemia reperfusion injury. Br J Pharma 2011; 162: 897-907.
24. Liu L, Chen C, Gong W, et al. Epoxyeicosatrienoic acids attenuate reactive oxygen species level, mitochondrial dysfunction, caspase activation, and apoptosis in carcinoma cells treated with arsenic trioxide. J Pharm Exp Ther 2011; 339: 451-63.
25. Zhao G, Tu L, Li X, et al. Delivery of AAV2-CYP2J2 protects remnant kidney in the 5/6-nephrectomized rat via inhibition of apoptosis and fibrosis. Hum Gene Ther 2012; 23: 688-99.
26. Liu Y, Lu X, Nguyen S, Olson JL, Webb HK, Kroetz DL. Epoxyeicosatrienoic acids prevent cisplatin-induced renal apoptosis through a p38 mitogen-activated protein kinase-regulated mitochondrial pathway. Mol Pharm 2013; 84: 925-34.
27. Wu HF, Yen HJ, Huang CC, et al. Soluble epoxide hydrolase inhibitor enhances synaptic neurotransmission and plasticity in mouse prefrontal cortex. J Biomed Sci 2015; 22: 94.
28. Li J, Carroll MA, Chander PN, Falck JR, Sangras B, Stier CT. Soluble epoxide hydrolase inhibitor, AUDA, prevents early salt-sensitive hypertension. Front Biosci 2008; 13: 3480-7.
29. Jin MM, Zhang L, Yu HX, Meng J, Sun Z, Lu RR. Protective effect of whey protein hydrolysates on H_2O_2-induced PC12 cells oxidative stress via a mitochondria-mediated pathway. Food Chem 2013; 141: 847-52.
30. Monti J, Fischer J, Paskas S, et al. Soluble epoxide hydrolase is a susceptibility factor for heart failure in a rat model of human disease. Nat Genet 2008; 40: 529-37.
31. Huang H, Morisseau C, Wang J, et al. Increasing or stabilizing renal epoxyeicosatrienoic acid production attenuates abnormal renal function and hypertension in obese rats. Am J Physiol Renal Physiol 2007; 293: F342-9.
32. Abramova TO, Redina OE, Smolenskaya SE, Markel AL. Elevated expression of the Ephx2 mRNA in the kidney of hypertensive ISIAH rats. Mol Biol 2013; 47: 821-6.
33. Luo P, Chang HY, Zhang S, et al. Inhibition or deletion of soluble epoxide hydrolase prevents hyperglycemia, promotes insulin secretion, and reduces islet apoptosis. J Pharm Exp Ther 2010; 334: 430-8.
34. Jang JH, Surh YJ. Protective effects of resveratrol on hydrogen peroxide-induced apoptosis in rat pheochromocytoma (PC12) cells. Mutat Res 2001; 496: 181-90.
35. Cheng B, Lu H, Bai B, Chen J. d-β-Hydroxybutyrate inhibited the apoptosis of PC12 cells induced by H_2O_2 via inhibiting oxidative stress. Neurochem Int 2013; 62: 620-5.
36. Iijima T, Mishima T, Tohyama M, Akagawa K, Iwao Y. Mitochondrial membrane potential and intracellular ATP content after transient experimental ischemia in the cultured hippocampal neuron. Neurochem Int 2003; 43: 263-9.
37. Yang X, Wang Q, Wang C, Qin X, Huang Y, Zeng R. Synthesis and protective effects of kaempferol-3′-sulfonate on hydrogen peroxide-induced injury in vascular smooth muscle cells. Chem Biol Drug Des 2016; 87: 841-8.
38. Cai Y, Hu X, Yi B, Zhang T, Wen Z. Glucagon-like peptide-1 receptor agonist protects against hyperglycemia-induced cardiocytes injury by inhibiting high mobility group box 1 expression. Mol Biol Rep 2012; 39: 10705-11.
39. Iacobazzi D, Mangialardi G, Gubernator M, et al. Increased antioxidant defense mechanism in human adventitia-derived progenitor cells is associated with therapeutic benefit in ischemia. Antioxid Redox Signal 2014; 21: 1591-604.
40. Ray PD, Huang BW, Tsuji Y. Reactive oxygen species (ROS) homeostasis and redox regulation in cellular signaling. Cell Signal 2012; 24: 981-90.
41. Choi EO, Jeong JW, Park C, et al. Baicalein protects C6 glial cells against hydrogen peroxide-induced oxidative stress and apoptosis through regulation of the Nrf2 signaling pathway. Int J Mol Med 2016; 37: 798-806.
42. Forbes-Hernández TY, Giampieri F, Gasparrini M, et al. The effects of bioactive compounds from plant foods on mitochondrial function: a focus on apoptotic mechanisms. Food Chem Toxicol 2014; 68: 154-82.
43. Brunelle JK, Letai A. Control of mitochondrial apoptosis by the Bcl-2 family. J Cell Sci 2009; 122: 437-41.
44. Kuwana T, Bouchier-Hayes L, Chipuk JE, et al. BH3 domains of BH3-only proteins differentially regulate Bax-mediated mitochondrial membrane permeabilization both directly and indirectly. Mol Cell 2005; 17: 525-35.
45. Li J, Wang Y, Du L, et al. Radiation-induced cytochrome c release and the neuroprotective effects of the pan-caspase inhibitor z-VAD-fmk in the hypoglossal nucleus. Exp Ther Med 2014; 7: 383-8.
46. Jiang GB, Zheng X, Yao JH, et al. Ruthenium(II) polypyridyl complexes induce BEL-7402 cell apoptosis by ROS-mediated mitochondrial pathway. J Inorg Biochem 2014; 141: 170-9.
47. Zhu M, Li J, Wang K, Hao X, Ge R, Li Q. Isoquercitrin inhibits its hydrogen peroxide-induced apoptosis of EA.hy926 cells via the PI3K/Akt/GSK3β signaling pathway. Molecules 2016; 21: 356.
48. Mahata B, Biswas S, Rayman P, et al. GBM derived gangliosides induce T cell apoptosis through activation of the caspase cascade involving both the extrinsic and the intrinsic pathway. PLoS One 2015; 10: e0134425.
49. Zhou Y, Wang Q, Evers BM, Chung DH. Signal transduction pathways involved in oxidative stress-induced intestinal epithelial cell apoptosis. Pediatr Res 2005; 58: 1192-7.
50. Woodgett JR. Recent advances in the protein kinase B signaling pathway. Curr Opin Cell Biol 2005; 17: 150-7.

51. Juhaszova M, Zorov DB, Yaniv Y, Nuss HB, Wang S, Sollott SJ. Role of glycogen synthase kinase-3beta in cardioprotection. Circ Res 2009; 104: 1240-52.
52. Kim DE, Kim B, Shin HS, Kwon HJ, Park ES. The protective effect of hispidin against hydrogen peroxide-induced apoptosis in H9c2 cardiomyoblast cells through Akt/GSK-3β and ERK1/2 signaling pathway. Exp Cell Res 2014; 327: 264-75.
53. Linseman DA, Butts BD, Precht TA, et al. Glycogen synthase kinase-3beta phosphorylates Bax and promotes its mitochondrial localization during neuronal apoptosis. J Neurosci 2004; 24: 9993-10002.
54. Kaga S, Zhan L, Altaf E, Maulik N. Glycogen synthase kinase-3beta/beta-catenin promotes angiogenic and anti-apoptotic signaling through the induction of VEGF, Bcl-2 and survivin expression in rat ischemic preconditioned myocardium. J Mol Cell Cardiol 2006; 40: 138-47.
55. Karrasch T, Spaeth T, Allard B, Jobin C. PI3K-dependent GSK3β(Ser9)-phosphorylation is implicated in the intestinal epithelial cell wound-healing response. PLoS One 2011; 6: e26340.
56. Piotrowski J, Jędrzejewski T, Pawlikowska M, Pacuła AJ, Ścianowski J, Kozak W. The weakening effect of soluble epoxide hydrolase inhibitor AUDA on febrile response to lipopolysaccharide and turpentine in rat. J Physiol Biochem 2017; 73: 551-60.